

Improved CEST detection in frequency domain using the Length and Offset VARIation of Saturation (LOVARS-CEST) acquisition scheme

X. Song^{1,2}, A. A. Gilad^{1,2}, G. Liu^{1,3}, P. C. Van Zijl^{1,3}, J. W. Bulte^{1,2}, and M. T. McMahon^{1,3}

¹Division of MR Research, Russel H. Morgan Dept. of Radiology and Radiological Science, Johns Hopkins University, Baltimore, MD, United States, ²Cellular Imaging Section, Institute for Cell Engineering, Johns Hopkins University, Baltimore, MD, United States, ³F.M. Kirby Center, Kennedy Krieger Institute, Baltimore, MD, United States

Introduction:

In recent years many new applications has been suggested for Chemical Exchange Saturation Transfer (CEST) imaging^{1,2}, where the CEST contrast is produced by applying a RF saturation pulse on resonance with the exchangeable protons, with the saturation then transferred via the chemical exchange between the protons on the agent and bulk water leading to a loss in water signal. However, there are also other sources of water signal losses such as direct water saturation and also endogenous Magnetization Transfer (MT)³ of tissue which complicate the data analysis. Assuming that these other sources of contrast are symmetric around the water peak, the conventional way to detect CEST contrast is asymmetry analysis⁴. However, for *in vivo* imaging, most tissue has an inherent asymmetric MT component⁵. Additionally, a small shift in Z-spectra may also result in asymmetric signal loss. Both of these effects can not be differentiated from CEST contrast using asymmetry analysis. In this study we have developed a new method for separating the CEST and MT contrast after correcting for B₀ inhomogeneity, termed the Length and Offset VARIation of Saturation CEST (LOVARS-CEST).

Materials and Methods:

LOVARS Scheme: We have developed a new acquisition scheme to modulate the CEST contrast and MT contrast at different frequencies through varying the saturation as shown in Fig.1. Briefly, a series of images were collected with the Length and Offset VARIation of Saturation(LOVARS) scheme, where the image intensity along the acquisition series oscillates at different pattern for voxels with MT and CEST contrast. A schematic of this is shown in Fig.1b. The acquisition pattern consists of *n* groups of LU(LOVARS Unit): $[(\omega_{sat}=-\Delta\omega, t_{sat}=4s), (\omega_{sat}=\Delta\omega, t_{sat}=2.5s), (\omega_{sat}=\Delta\omega, t_{sat}=4s), (\omega_{sat}=\Delta\omega, t_{sat}=2.5s)]_n$, where ω_{sat} is the center frequency for the saturation pulse, t_{sat} is the saturation time and $\Delta\omega = 3.6\text{ppm}$ from water, so that the saturation pulse is either directly on resonance with the exchangeable protons in PLL, or at the same distance but on the opposite side of water.

Phantom: The phantom was constructed using 1-mm-diameter glass capillaries with: PLL (poly-L-lysine), a CEST contrast agent, agar gel to model MT contrast, and 1mM PBS to represent cerebral spinal fluid. PLL and Agar were dissolved in PBS over the range of concentrations mentioned in Fig.1, Table1. All capillaries were mounted in a holder with their positions illustrated in Fig.1a and kept at 37°C during the image acquisition. All the PLL samples were titrated to PH 7.3.

Image Acquisition: All images were acquired on a 11.7T Bruker Avance spectrometer with a 15mm birdcage RF coil. The imaging sequence consists of a saturation pulse of 4.7 μT RF power and the RARE pulse sequence (RARE factor =16). Other imaging parameters were: FOV=1.1x1.1cm, matrix size 128x64, slice thickness 0.5mm, and TR/TE=6000/4.9ms. In Fig 2b, n=2, but the pattern could be repeated more times to improve the SNR. We acquired three sets of LOVARS images using three positive ($+\Delta\omega=3.6, 3.5, 3.3\text{ppm}$) and three negative offset frequencies ($-\Delta\omega=-3.6, -3.7, -3.9\text{ppm}$) to correct the images according to the map generated by Water Saturation Shift Referencing (WASSR)⁶.

Post processing: 1) Based on the map of water frequency shift, a voxel-by-voxel Z-spectra shift correction was performed by interpolating the intensity of the three sets of images at different offset frequencies⁷. 2) Using the two offset values (-3.6, 3.6ppm) of the shift-corrected data, for each voxel, the intensity waveform along the image series was transformed to the frequency domain by a Fast Fourier Transform. 3) In the frequency domain, voxels were differentiated according to their frequency of the maximum magnitude: voxels with CEST contrast possess the peak value of frequency spectrum at one modulation frequency (called $f(\text{CEST})$), while voxels with MT contrast has another peak frequency, called $f(\text{MT})$ (Fig. 1c). 4) After voxel-classification, select voxels of CEST contrast and generate the FFT magnitude map at $f(\text{CEST})$ shown in Fig. 1d, where the FFT magnitude is proportional to $MTR_{\text{asym}} = (S^{-\Delta\omega} - S^{+\Delta\omega}) / S^{-\Delta\omega}$. In the same way, an MT contrast map can be produced (Fig.1e).

Results and Discussion:

We have acquired images using our new LOVARS scheme on a mixed phantom with capillaries, where both CEST and conventional MT contrast are displayed using the frequency filtered LOVARS images at $f(\text{CEST})$ (Fig. 1d) and $f(\text{MT})$ (Fig.1e). In Fig. 1d, only capillaries with the CEST contrast show up with the colormap indicating the MTR_{asym} value. Under the exact same experimental conditions, we collected 4 groups of $[S_w^{-\Delta\omega}, S_w^{+\Delta\omega}]$ with $t_{sat}=4s$, and display the resulting MTR_{asym} image in Fig.2 for comparison with our new method. The new LOVARS method can differentiate PLL from agar capillaries, unlike the simple MTR_{asym} maps. Table 1 further shows the quantitative comparison of the MTR_{asym} value and the intensity of FFT magnitude map at $f(\text{CEST})$ obtained by LOVARS. For the CEST contrast agent PLL, the LOVARS method can get almost the same value as the conventional MTR_{asym} , which indicates that the image of CEST contrast is quantitative. However, for agar capillaries which simulate MT effect, the conventional asymmetric analysis also display MTR_{asym} contrast (Even the lowest concentration, 1% agar, has a MTR_{asym} value of 0.043), while the LOVARS methods differentiate PLL and agar capillaries clearly.

Conclusion:

In summary, we developed a new way to differentiate CEST from conventional MT contrast through a new modulation scheme. It is well suited to distinguish CEST from non-CEST contrast, and thus can reduce the minimum detectable CEST contrast. Additionally, this technique can acquire quantitative CEST and MTR images simultaneously. This new method can potentially improve the detection of small amounts of CEST agent *in vivo*.

Reference: 1. Sherry, A.D. et al., Annu. Rev. Biomed. Eng. 2008. **10**: 391-411. 2. Zhou, J. et al., Prog. Nucl. Magn. Reson. Spectrosc., 2006. **48**(2-3): 109-136. 3. Henkelman, R. M. et al., NMR Biomed 2001. **14**: 57-64. 4. Ward, K. M. et al., J. Magn. Reson. 2000. **143**: 79-87. 5. Pekar, J. et al., MRM,1996. **35**:70-79. 6. Kim, M. et al., MRM, 2009. **61**: 1441-1450. 7. Zhou, J. et al., MRM,2008. **60**: 842-849

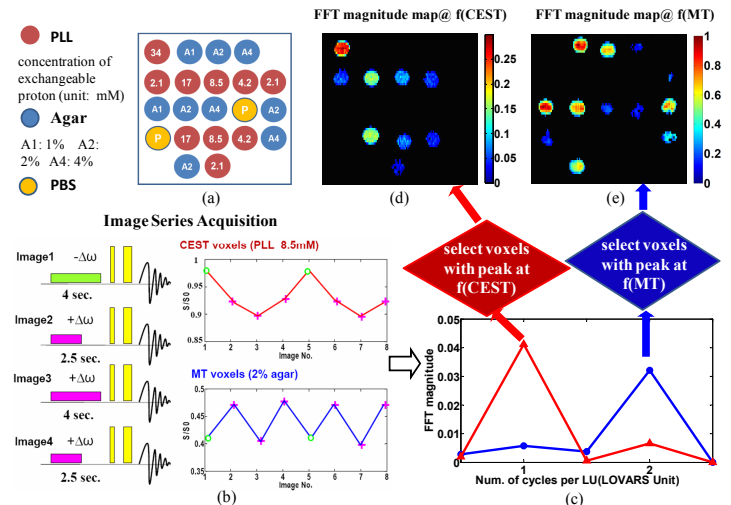


Fig.1 Illustration of LOVARS procedure for achieving CEST and MT contrast map

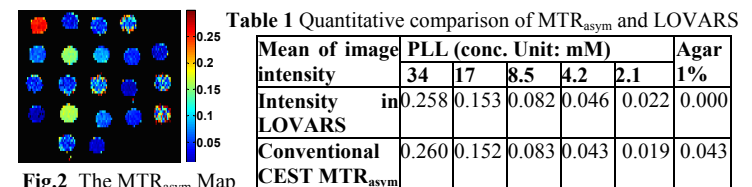


Fig.2 The MTR_{asym} Map

Table 1 Quantitative comparison of MTR_{asym} and LOVARS

Mean of image intensity	PLL (conc. Unit: mM)					Agar
	34	17	8.5	4.2	2.1	1%
Intensity in LOVARS	0.258	0.153	0.082	0.046	0.022	0.000
Conventional CEST MTR_{asym}	0.260	0.152	0.083	0.043	0.019	0.043